Indian Journal of Chemical Technology
Vol. 31, January 2024, pp. 70-84
DOI: 10.56042/ijct.v31i1.1719

Fabrication of novel magnetic graphene oxide nanoadsorbent from *Strychnous potatorum* seeds for enhanced removal of chromium from wastewater

R. Janani[1], K. Sivakumar[2] & G. Baskar[1]*

[1]Department of Biotechnology, St. Joseph's College of Engineering, Chennai- 600 119, Tamil Nadu, India

[2]Department of Biotechnology, Karpaga Vinayaga College of Engineering & Technology, Chinna Kolambakkam-603 308, Tamil Nadu, India

*E-mail: basg2004@gmail.com

Received 19 May 2023; accepted 12 December 2023

The main aim of the study is to synthesize graphene oxide from natural source (by utilizing *Strychnous potatorum* seeds) and composite with iron oxide to form magnetic graphene oxide (MGO) which has been applied as adsorbent for removal of chromium from wastewater. The prepared MGO adsorbent has been characterized by FTIR, XRD, VSM, UV-visible and SEM to examine its structural, morphology, elemental and chemical composition. The average particle size of MGO from SEM image is 47.2 nm and analysis results show the successful oxidation of GO and well distribution of magnetic iron oxide particles onto GO. Batch method has been opted for adsorption process and the operation parameters are optimized. The adsorbent MGO exhibits maximum removal rate of 97.1% for chromium under optimized conditions. An adsorbent dose of 10 mg shows maximum efficiency in the adsorption process. Adsorption Isotherm and kinetic behaviour are investigated and founded that Freundlich adsorption isotherm model are well suited for chromium (R^2=0.996) and the adsorption behaviour are well explained by pseudo second order which followed by chemisorption. The maximum adsorption capacity (q_{max}) exhibited by this novel MGO adsorbent is 9.09 mg/g. Desorbing agent NaOH is used for desorption process. Only 17.1% efficiency is reduced even after 5 cycles of adsorption-desorption and proved can be reuse. This novel MGO adsorbent is easily separated after the adsorption process. From the study, it is concluded that this neoteric MGO adsorbent as a promising, super-eminent candidate for wastewater treatment.

Keywords: Adsorption kinetics, Graphene oxide, Green synthesis, Magnetic nanoadsorbent

Introduction

Healthy environment consists of pure water, clean air and nourishing soil[1]. Human depends on the environment for food, water, fuel, medicines and materials to build and other things. The development in science and technology gives both benefits and accomplished with abominable pollution for our environment. Water deterioration is utmost important issue facing by the entire world[2,3]. Water is the gift from nature, essential fuel to all living being and with its availability, life on the earth persistence. The water pollution is due to the disposal of toxic containing heavy metals like chromium, arsenic, lead, mercury, nickel and cadmium[4,5] in the form of waste water from the industries into natural water bodies, which largely pollute the water apart from domestic and agricultural waste water. They can easily pass through the food chain and cause serious diseases and malfunctions. Therefore, supply of clean and pure water is the biggest challenge faced by developing countries.

Among these toxic metals, chromium is one of the toxic metal ions which are highly reactive, amphoteric in nature and most toxic heavy metal among top pollutant list, by dint of its environmental endurance and non-eco friendly nature[6,7]. The two forms of chromium are Cr^{6+} and Cr^{3+} which are in stable oxidation state. Among them Cr^{6+} is highly toxic and its mobility nature results in diseases and malfunction in human health[8,9]. These ions are released by industries like leather tanning, electroplating, steel industries, petroleum refining process, paints and pigments, metal ceramics[10,11]. These industries emit nearly 2000-5000 mg/L of Cr^{6+} into water bodies[12], but the permissible limit of Cr^{6+} in industrial waste water are 0.25 mg/L whereas 0.05 mg/L for drinking water and 0.1 mg/L for surface water bodies, by WHO (world health organization)[11,13]. High level of these noxious metal ions in wastewater needs to be stepped down to acceptable level.

For cleanup of wastewater, the most widely accepted method is adsorption because of its

economical, ecofriendly, and efficacious nature[14,15]. The selection of right adsorbent for process of adsorption was a big deal. Over traditional adsorbents carbon based adsorbents gained more attention[16]. Carbon based adsorbents are in the hit list of researchers, among them graphene is an interesting material which is a 2D crystal with one atom thick with unique properties like large surface area, excellent mechanical properties, good electrical, optical, and enhanced thermal properties. Graphene is nonpolar and hydrophobic in nature with good chemical stability[2,17]. Graphene oxide (GO) which is oxidation product of graphene, is polar and hydrophobic in nature, with oxygen containing functional groups like hydroxyl, epoxy, carbonyl groups which makes its easy disperse in aqueous solution[14,25]. GO was synthesized from natural sources like tea waste, coconut fronds, coconut shell, sugarcane dry leaves, water hyacinth root, oil palm-based waste and natural and industrial carbonaceous waste[15-21], but there was a difficult to separate it out after its use. So, combining with magnetic material like Fe_3O_4, separation of it after using as an adsorbent can be easily performed with magnets and are called as magnetic graphene oxide (MGO). Fe_3O_4 have positive effects with low toxicity and used for many pollutants in wastewater treatment as reported by various researchers.[23,24,26,27]

Many researchers have reported that MGO was often synthesized using synthetic graphite as the source[24,26]. In this study, MGO was prepared from *Strychnous potatorum* seeds as a natural source. To the foremost of our knowledge this seed was so far not reported in the synthesis of MGO. *S. potatorum* seeds are native of India, especially southern parts of Tamil Nadu and called as 'nirmali' tree as the name implies 'nir' means 'no' and 'mali' means 'impurities. The seeds are called as clearing nut seeds in English; the thankotai in Tamil language. The seeds and leaves are showing excellent medicinal properties and possess wonderful cleansing properties, as over many decades, this seed was used in rural community to clean the water. These seeds reported to adsorb metal ions and even to treat nuclear wastes, and also remove dyes and are used for biogas production too[28]. Many researchers have reported the coagulant property of this seeds and no toxicity is recorded[29,30]. Nearly 4000 years ago there was a practice of cleaning the water using these seeds and even now in practice of using these seeds in southern parts of Tamil Nadu[31]. The polysaccharide content of these seeds were extracted and made in form of hydrogel which was used as chemotherapeutics and for antimicrobial applications[32]. Seed possess excellent purification properties even without modification. Widely available nature and non-toxic nature, eco friendliness were the reasons behind the selection of this seed for the study. These valuable points, provoke an idea of enumeration of GO an excellent material and wonderful sorbent from this super eminent seed and this GO was magnetized for ease of separation.

In this research work, a neoteric and efficient GO was synthesized by utilizing *S. potatorum* seeds as natural source. Further, GO was composited with iron oxide to form MGO and this novel MGO has been used for the removal of chromium from wastewater. Specific objectives of the study: (1) to find the structural, morphological, elemental and chemical composition of synthesized MGO, using techniques like VSM, XRD, FTIR, UV-visible and SEM, (2) to test the adsorption performances of the novel MGO, and optimization of influencing factors like time, dose, pH, temperature and concentration, (3) to find the adsorption behaviour of fabricated MGO, using various isotherm and kinetic models and (4) desorption behaviour of the fabricated nanocomposite for its effective reuse.

Experimental Section

Materials

Potassium permanganate ($KMnO_4$), sulfuric acid (H_2SO_4), phosphoric acid (H_3PO_4), hydrogen peroxide (H_2O_2), sodium nitrate ($NaNO_3$), hydrochloric acid (HCl), ethanol, ether, sodium hydroxide (NaOH), iron(III) chloride hexahydrate ($FeCl_3 \cdot 6H_2O$), iron(II) sulfate heptahydrate ($FeSO_4 \cdot 7H_2O$), potassium dichromate ($K_2Cr_2O_7$), nickel(II) nitrate hexahydrate were purchased with analytical grade and highest purity. The *S. potatorum* seeds were purchased from local shop, Chennai, India. Hanna hand held pH meter (HI-9124), United states, Shaker (Agile) was used for measuring the pH.

Preparation of graphite from *Strychnous potatorum* seeds

Seeds were washed thoroughly using tap water. Then seeds were heated to 105°C by using oven and left at the same temperature for 5 h to dehydrate the moisture content. After that, the dehydrated seeds were undergone carbonization process for 30 min at 400°C. This carbonized material was crushed using a mortar, sieved and used as natural graphite for the preparation of graphene oxide[23].

Synthesis of graphene oxide using natural graphite from *Strychnous potatorum* seeds

Graphene oxide was synthesized by modified Hummer's method[33] using the natural graphite obtained. Initially, 3 g of obtained graphite was added to 18 g of potassium permanganate (3:6 %, *w/w*) to sulphuric acid and phosphoric acid mixture in the ratio of 360:40 ml (9:1 *v/v* %) under ice bathcondition. This suspension is accompanied by slightly exothermic reaction at 35-40°C. The solution was turned to purple brown in colour and continued stirring for 12 h at 50°C in a temperature controlled condition. After that the suspension turned to dark brown indicating the oxidation of graphite. Then the solution was cooled and 400 mL of ice-cold distilled water was added, in order to avoid overheating and decrease the viscosity. Then 9 mL of hydrogen peroxide was added in 30 %, *v/v* ratio to remove the metal salts and permanganate residues from the mixture, as a result the solution turned to bright yellow colour. Then this solution was centrifuged for one hour at 1500 rpm and the supernatant was decanted. The remainder was rinsed three times with different solutions. First rinsed with 200 mL of deionized water, and then with 200 mL 30%(v/v) of hydrochloric acid and finally with ethanol. After each rinse the suspension was centrifuged for 2 h at 4000 rpm and supernatant was decanted. After three times of rinse, to the add 40 mL of ether was added to the remainder, coagulated and filtered. The obtained solid material was vacuum dried to obtain graphite oxide in powder form. This graphite oxide was ultrasonicated with distilled water to obtain the GO.

Synthesis of magnetic graphene oxide using graphene oxide from *Strychnous potatorum* seeds

This magnetic material was synthesized using a method followed by Neolaka et al.[23] in 2020. Initially 0.025 g of graphite oxide was ultra-sonicated for 30 min with distilled water to obtain GO. The iron oxide solution was prepared separately with 0.556 g of iron(II) sulfate heptahydrate and 1.081 g of iron(III) chloride hexahydrate salts were mixed and stirred up to 30 min at temperature 40°C. The pH was set to be 4.0 by 1 M sodium hydroxide. Now, iron oxide solution was added to the mixture of sonicated GO solution and stirred for 30 min. Then the solution was changed to its pH 10.0 with 1 M sodium hydroxide and continued stirring for 30 min. A black precipitate resulted was separated from the solution by using magnets. Then, the obtained magnetic material was washed with deionized water and methanol and dried at 60°C for 24 h to obtain powdered form of MGO.

Characterization of adsorbent

The prepared nanomaterial was undergone various characterization. The XRD pattern was observed on X-ray diffractometer (PANalytical, Netherlands) at a wavelength of 1.514 Å with voltage 40 kV and current 30 mA in 2θ range from 5° to 80° by using step scan mode. The existing functional groups were recorded by FTIR (SHIMADZU IR TRACER 100, America) with KBr pellet in the wavenumber range 400-4000 cm^{-1}. The magnetic properties of the prepared MGO was observed with VSM (vibrating magnetometer, Lake shore, United states) at room temperature. The morphology of the prepared magnetic graphene oxide was analyzed by SEM (scanning electron microscope) with FEI quanta FEG 200 microscopes. UV-visible absorption spectrum of MGO was recorded by UV-visible spectrophotometer (SHIMADZU UV 3600 PLUS, America).

Adsorption experiment

Batch method was opted for optimization of parameters of adsorption of chromium ions on to the surface of MGO nanoadsorbent. Initially start with the parameter of contact time (10, 20, 30, 40, 50, 60, 70, 80 min) with different intervals, adsorbent dosage (varying amount of 10, 20, 30, 40, 50 mg/100 mL), metal ion concentration (10, 20, 30, 40, 50 mg/L), varying pH (2.0-10.0) and temperature (20-70°C). At different conditions the prepared samples were exposed to adsorbent MGO surface and after the equilibrium time the adsorbent was removed using external magnet and the samples were filtered and analyzed for the metal ion concentration. Hence, optimum parameters were determined from the experiment and the adsorbent capacity and percentage removal efficiency was calculated using Eqs (1) and (2);

$$Qe = (c_o - c_e) * \frac{v}{m} \quad \ldots(1)$$

$$\%R = \left[\frac{c_o - c_e}{c_o}\right] * 100 \quad \ldots(2)$$

where, Qe is amount of metal ion adsorbed at equilibrium conditions (mg/g), c_o is initial metal ion concentration, c_e is equilibrium concentration of the metal ion, V is the volume of metal ion solution (mL) and m is mass of adsorbent used (mg).

Adsorption isotherms study

Adsorption isotherm study was tested with different metal ion concentration in the range of 10-100 mg/L with 20 mg adsorbent dose for 50 mL of metal ion solution and kept in mechanical shaker for optimum time. The residual concentration of metal ion was analyzed after removing the adsorbent by external magnet and filtered. By using the obtained equilibrium data from the process, there are many isotherm models used by researchers to predict the adsorption process occurred on the adsorbent surface by the metal ion. In our study Langmuir, Freundlich and Temkin isotherm models were tested for fitness with the obtained data and also to predict the best fit among them and their equation were tabulated in Table 1.

Langmuir isotherm is a two-parameter model and explains about the formation of monolayer of adsorption on homogenous surface with equal energy for all adsorption sites and there was no trans immigration of adsorbate metal ion on to the surface[34,35]. Freundlich isotherm is multifaceted adsorption occurred on heterogeneous surface. This model describes the relationship of adsorbed metal ions which travels from liquid to solid surface and possess numerous sites with assorted energies and for large range of adsorption data, this model is not valid. Temkin model indicates indirect interaction MGO nanoadsorbent in the adsorption process and assumed to be when there is a decrease in the heat of adsorption on the molecules in the adsorption layer occur which results in increase in the surface coverage.

Adsorption kinetics study

Adsorption kinetic study was carried out at different interval of contact time from 15-150 min with 20 mg adsorbent for 50 mL of metal ion solution and kept in mechanical shaker for optimum time. The residual concentration of metal ion was analyzed after removal of adsorbent by external magnet and filtered. With the obtained adsorption data there were different kinetic models used to predict the adsorption process occurred on the metal ion to the MGO surface.

In our study pseudo first order (PFO), pseudo second order (PSO) and Intraparticle diffusion model (IPD) were fitted to the obtained data to predict the best fit among them and their equation was tabulated in Table 2. Lagergren based pseudo first order model is valid for lower concentration ranges and states that adsorption kinetics are proportional to the number of adsorption sites which is also reciprocal to the concentration of the metal ion whereas the pseudo

Table 1 — Isotherm Models equations and their parameters

Isotherm model equations	Parameters
Langmuir isotherm $q_e = \frac{q_m K_L C_e}{1 + K_L C_e}$ $\frac{1}{q_e} = \frac{1}{q_m} + \left(\frac{1}{K_L q_m}\right) * \left(\frac{1}{C_e}\right)$ $R_L = \frac{1}{1 + K_L C_o}$	q_e is the amount of metal ion adsorbed at equilibrium conditions (mg/g), C_e is the equilibrium concentration of the metal ion (mg/L), q_m (mg/g) is the maximum amount of adsorbed metal ion per unit mass of sorbent, K_L (L/mg) is the Langmuir constant R_L is a separation factor The R_L value says about the shape of the isotherms: if > 1 it is unfavourable; it is linear when its =1; and it is favourable only when the value lies between 0-1
Freundlich isotherm $q_e = K_F C_e \frac{1}{n}$ Logarithmic form: $lnq_e = lnK_F + \frac{1}{n} lnC_e$	K_F and n are the indicates the adsorption capacity and intensity of the adsorbent The degree of nonlinearity between the quantity adsorbed and the solution concentration was given by adsorption intensity (n) as follows: When n=1, the adsorption process is linear, when n>1, it is physical; when n <1 it is chemisorption ; when the n value is lies 1-10, best fit.
Temkin isotherm $q_e = \frac{RT}{b} \ln (k_m c_e)$ Linear form: $q_e = \frac{RT}{b} lnk_m + \frac{RT}{b} lnC_e$	b is Temkin constant which is related to the heat of sorption (J/mol), R is universal gas constant, K_T is Temkin isotherm constant (l/g)

Table 2 — Kinetics model equations with parameters

Sl. No.	Kinetics model equations	Parameters
1.	Pseudo first order $\frac{dq_t}{dt} = k_f(q_e - q_t)$ Integration form: $ln(q_e - q_t) = lnq_e - k_f t$	q_t is the amount of metal ion adsorbed at time t (mg/g), k_f is the rate constant (min), t is the time (min)
2.	Pseudo second order $\frac{dq_t}{dt} = k_2(q_e - q_t)$ Integration form: $\frac{t}{q_t} = \frac{1}{k_2 q_e^2} + \frac{t}{q_e}$	$k_2$is the second order rate constant (g/mg min), q_e is the maximum adsorption capacity of the adsorbent in mg/g, q_t (mg/g) is the amount of adsorption occurred at time t.
3.	Intraparticle diffusion $q_t = k_p t0.5 + C$	q_t (mg/g) is the amount of solute molecules adsorbed onto the sorbents for a given time t, k_p (mg/g min 0.5) is the rate constant, C is the intercept.

second order assumes that adsorbent active sites are proportional to the adsorption process. Intraparticle diffusion model depicts about the diffusion mechanism occurred between the sorbent and solute molecules, and also finds the rate limiting step of the adsorption process[36].

Desorption and regeneration study

This study was done to find the reusability of the MGO nanoadsorbent in the economic view point and to find its potency of stability over many cycles. For this study, 20 mg of MGO was loaded with 50 mg/L concentration of each metal ion and after reaching equilibrium at 80 minutes, the adsorbent was separated and the residual concentration was analysed and then the adsorbent was dried in oven at 60°C. For desorption this dried adsorbent was used. The different concentrations of regenerants were evaluated and selected 1 M NaOH for the study. These regenerants were treated with the metal loaded adsorbent. After desorption the adsorbents were separated, washed, dried and reused for another cycle of adsorption-desorption. Similarly, five cycles were done to find its efficiency[37].

Results and Discussion

Characterization of MGO nanoadsorbent

The prepared MGO nanoadsorbent was characterized for its functional group by FTIR. Fig. 1 shows the FTIR spectrum of MGO which consists of the characteristic peaks at 553.57 cm^{-1} are attributed to Fe-O stretching vibration and this was due to the successful loading of Fe_3O_4 onto GO sheets. Two peaks at 879.54 and 1639.29 cm^{-1} are assigned to C=C stretching vibrations and the peak at 1639.29 cm^{-1} arises due to natural graphite from *S. potatorum* seeds

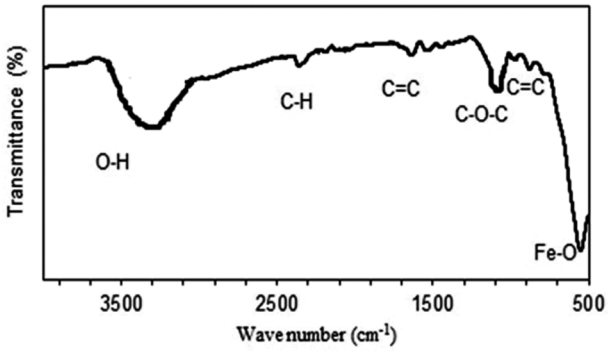

Fig. 1 — FTIR spectrum of synthesized MGO nanoadsorbent

which not completely oxidizes, Neolaka et al. [23], studied the enumeration of graphene oxide from kesambi wood as natural source and reported the occurrence of this peak rise at same wavenumber. O-H group was observed at 3251 cm^{-1} which also confirmed the successful anchoring of Fe_3O_4 on to GO sheets. A stretching of vibration of C-O-C band of GO was observed at 1105.4 cm^{-1}. From the FITR spectrum it is confirmed that iron oxide particles successfully anchored on GO sheet and this fabricated MGO contains hydroxyl, oxygen, carbon containing functional groups which are responsible for metal co-ordination to the binding sites of adsorbents and paves way for elimination of metal ions from wastewater.

Fig. 2 shows the XRD plot obtained for MGO. The diffraction peaks obtained at 2θ = 9.8°, 18.3°, 30.2°, 35.6°, 43.5°, 53.7°,57.1°, 62.8°, 66.2°, 74.1°, 89.8° with its corresponding miller indices were (001), (111), (311), (400), (422), (511), (440), (533), respectively. Neolaka et al. [23] and Hieu et al. [38] were also mentioned the related diffraction peaks in their work of synthesized MGO from different natural sources. The peak at 9.8° corresponds to the

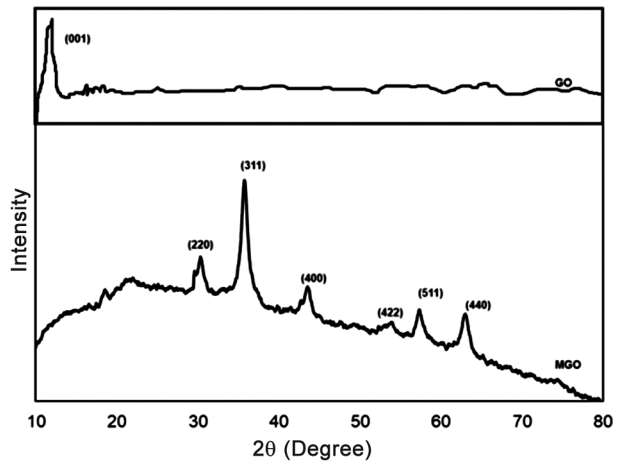

Fig. 2 — X-ray diffractogram of GO and synthesized MGO nanoadsorbent

formation of oxygen containing functional group in the graphite. Hoan et al.[39] reported that this peak was at 11.8º in his study, due to their preparation procedure. They also reported that appearance of peak at 26º and claimed that it was due to the incomplete oxidation of graphite sheets. Here, in this study absence of such peaks due to the efficiency of our procedure, which show successful oxidation of graphite. The rise of diffraction peaks at 43.5, 53.7, 57.1, 62.8°, confirms the loading of iron oxide to GO sheets. Neolaka et al. [23] reported the synthesis of MGO from *Kesambi* wood as natural source and also reported that this rise of peaks indicates the iron oxide loaded onto GO sheets. The characteristic peaks for iron oxide nanoparticles were 30, 35, 43, 53, 57 and 62º and this was from JCPDS file card number 19-0629, which shows that *S. potatorum* seed made MGO material contains magnetic iron oxide and the crystal is face centred cubic. The crystal size measured using Scherrer's equation:

$$D = \frac{K\lambda}{\beta COS\theta}$$

Where D is crystal size in nm, K=Scherrer constant (0.9), λ=wavelength (0.15406 nm), β=FWHM (full width at half maximum) position (radians), θ=peak position (radians). The crystal size of MGO nanocomposite calculated using Scherrer equation is 18.09 nm.

The magnetized carbon materials have great attention towards water remediation because of their efficiency and easy separation[26]. VSM at room temperature was measured to finds the magnetic property of the prepared MGO adsorbent. The

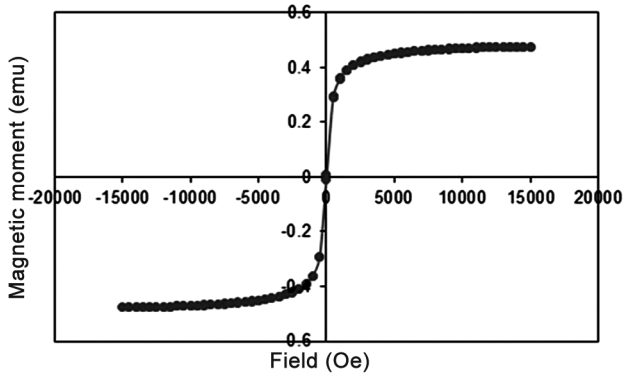

Fig. 3 — Magnetic hysteresis loop (M-H) of synthesized MGO nanoadsorbent

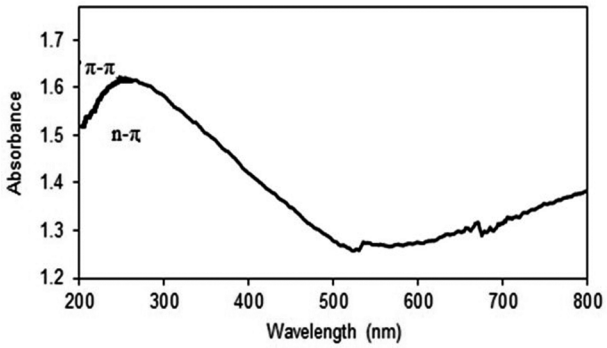

Fig. 4 — UV-visible absorption spectrum of synthesized MGO nanoadsorbent

magnetic hysteresis loop of MGO was obtained at RT as shown in the Fig. 3 and it looks like s-like curve. The absences of hysteresis loop leads to confirm the super paramagnetic nature of fabricated MGO[40], also the low remanence and coercivity value of the curve proves the same[23]. The saturated magnetization (Ms) of MGO was 47.616 emu/g. This value is strong enough for magnetic separation of adsorbent after the adsorption process. This value is higher compared to literatures [24,38,39,41]. Successful incorporation of magnetic nanoparticles into GO sheets reflects in the obtained VSM results.

Uv-visible absorption spectrum of MGO is shown in Fig. 4. The spectra exhibit peak at 248 nm which represents for π-π transition of aromatic carbon bonds (C=C) on the surface of MGO. It was also the characteristic peak for GO and peak at 288 represents for n-π transition of deduced carbonyl groups(C=O) and also stated that covalent attachment of Fe_3O_4 onto GO sheets.

The morphology and elemental compostion images of prepared magnetic graphene oxide are shown in Fig. 5 (a,b) and (c,d), respectively. From the SEM image (Fig. 5a & b), it is evident that magnetic iron

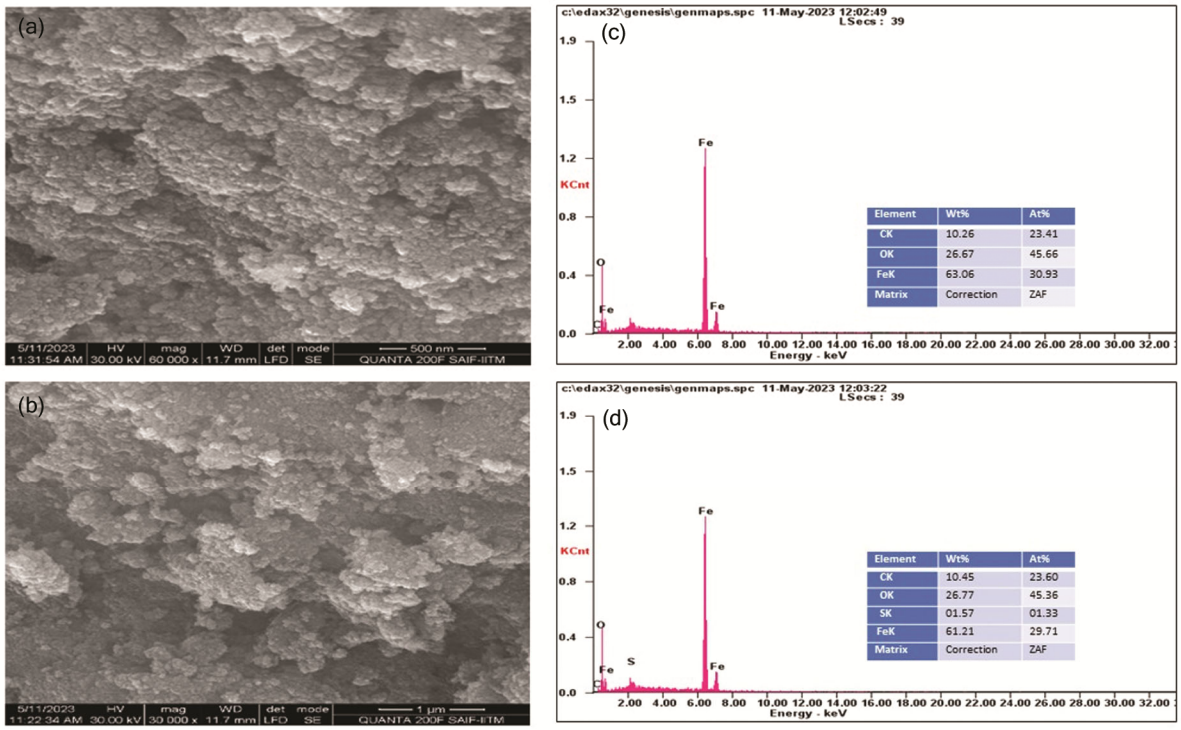

Fig. 5 — (a,b) SEM images of MGO and (c,d) corresponding elemental composition graphs

oxide particles were well distributed on the surface of GO sheets. The average particle size of MGO is 47.2 nm. The EDX spectrum shows the major consitiuent elements are oxygen (47 at.%), carbon (23.41 at.%), and iron (32.67 at.%). These results confirms sucessful oxidation of GO sheets and also anchoring of iron oxide particles onto GO sheets. There were very small hydrogen containing functional groups attached to the basal plane of GO sheets which was undectable as because of its lower atomic mass.

Optimization of process parameters for adsorption chromium using MGO nanoadsorbent

In batch adsorption, contact time is an important factor which provides the information about sorption kinetics of the metal ions for adsorbent load. Even this does not provide accurate information for continuous process still it provides information about adsorption performance of the adsorbent. Adsorption process of contact time was studied from 10-80 min by keeping other parameters constant. The removal efficiency (R%) of chromium ions is shown in Fig. 6(a). For chromium ions maximum adsorption occurred at 50 min, of contact of time. The maximum adsorption shown by the chromium ions onto MGO surface was 2.96 mg/g. By increasing contact time, the adsorption of chromium ions reaches 97.1% at maximum for 50 mins of equilibrium time.

The efficiency of prepared MGO adsorbent was studied with different amount of doses from 10 to 50 mg. Maximum removal of chromium ions was found to be 98.49% obtained using 10 mg of dose and the q_{max} achieved was 3.59 mg/g. For chromium ions, there was a decrease in adsorption rate observed by improving (MGO) dose. This was owing to the aggregation of nanoadsorbent (MGO) which created lack of availability of binding sites[23]. The maximum removal efficiency of chromium with its adsorption capacity is shown in Fig. 6(b).

Concentration of metal ion investigated was in the range 10-50 mg/L, with 10 mg of MGO dose at room temperature for 50 min of contact of time. The maximum removal efficiency obtained was 99.3% with q_{max} of 4.26 mg/g. This removal rate was achieved for 10 mg/L concentration of chromium. Further increasing the concentration, the removal efficiency was decreased and reached to 88.3% at 50 mg/L of concentration. The maximal removal was acquired with the 10 min of exposure, the reason behind this is, at lower concentration initially metal ions binds rapidly and occupied the specific binding sites, and by increasing concentration the binding sites present on the MGO surface were occupied and saturated, with no sites for further binding[34,42]. Fig. 6(c) shows the maximum

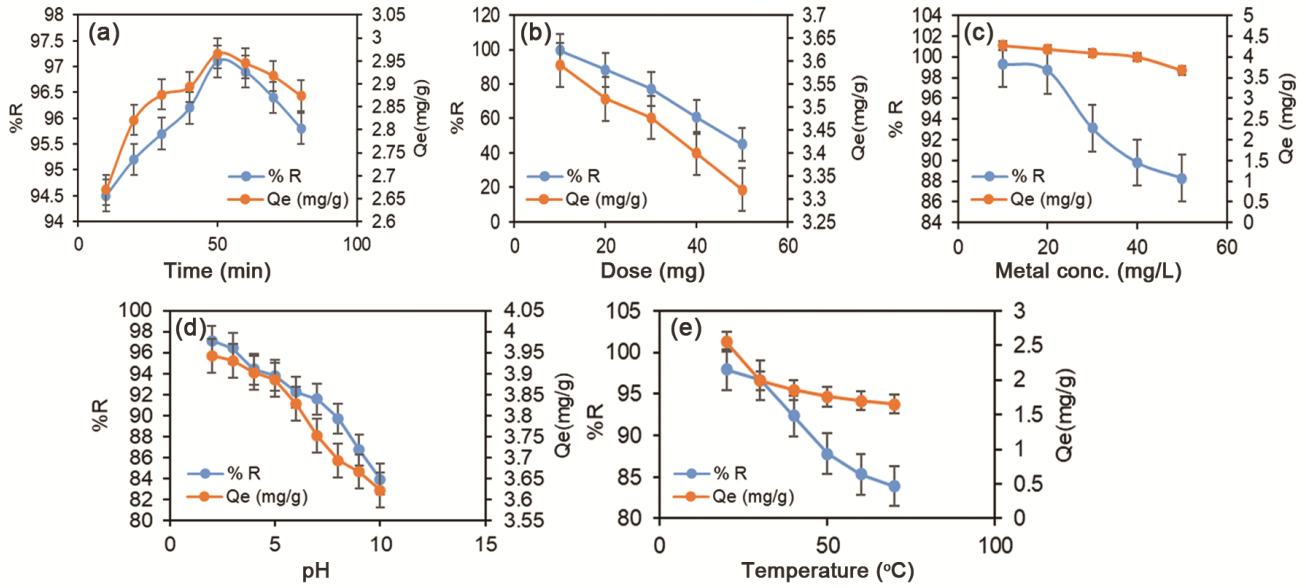

Fig. 6 — Optimisation parameters through batch adsorption: (a) Effect of contact time, (b) dosage, (c) concentration, (d) pH and (e) temperature

removal efficiency of chromium for different concentration with q_{max}.

The efficiency of pH plays a key role in the adsorption process. The pH evaluated in range from 2.0 to 10.0, with 10 mg/L of concentration of metal ion and 10 mg of MGO dose per 50 mL, under optimum time obtained previously. At pH 2.0, maximum adsorption was achieved with 97.12% of adsorption efficiency and adsorption capacity acquired was 3.94 mg/g. Many researchers have reported that pH 2.0 was ideal for maximum adsorption of chromium with different adsorbents[43-46]. The difference forms of chromium ions are $Cr_2O_7^{2-}$, $HCrO^{4-}$, $Cr_3O_{10}^{2-}$ and $Cr_4O_{13}^{2-}$ were dominantly present in the pH range of 1.0-6.0. So, at acidic conditions, the H^+ ion was protonated on MGO surface, due to electrostatic attraction force betwixt the MGO adsorbent surface and chromium metal ions adsorption occurs[47]. At higher pH, the dominant species $HCrO^{4-}$ will be changed to $Cr_2O_7^{2-}$, CrO_4^{2-}, which forms chromic acid ($H_2Cr_2O_7$). This leads to protonation of OH^- ions present in the surface of the MGO adsorbent, as a result there observed decrease in adsorption rate by means of electrostatic repulsion force. The reasons behind maximal adsorption attained by various researchers are, at alkaline pH, hydroxyl group get precipitated which leads to maximum adsorption rate[42]. Also at this pH, formation of metal complexes occurred either by precipitation, bonding or electrostatic attraction or repulsion force[48]. Removal efficiency of the metal ions with maximum adsorption capacity is depicted in Fig. 6(d).

Different temperature ranges from 10 to 70ºC was studied by keeping other parameters constant. From Fig. 6(e), it can be clearly perceived that by increasing temperature, removal rate of chromium was decreased. Herein, low temperature favours higher adsorption capacity. Maximum adsorption of chromium ions is 97.9% achieved at 20°C and it gradually decreases through increase in temperature and lowers to 84.7% at 70°C. The q_{max} acquired is 2.55 mg/g.

Kinetics of adsorption using MGO nanoadsorbent

Kinetic study reveals the rate controlling phase reaction and interaction of adsorbent mechanism in the adsorption process[49,50]. It also explains whether the rate controlling is mass transfer or chemical reaction[51]. To test the experimental data, pseudo first order, pseudo second order and intra particle diffusion were analysed. The kinetic plots of chromium are given in Fig. 7 and their corresponding calculated parameters are tabulated in Table 3. According to the obtained results, pseudo second order has attained highest correlation coefficient factor (R^2) 0.992 by chromium ions and showed best fit towards adsorption. The results showed that both the metal ions exhibit chemisorption driven adsorption process which occurred by the binding sites on the surface of

the MGO nanoadsorbent and the interactions of electrons occurred in the solution towards adsorbent[23].

The pseudo first order and pseudo second order can not describe the mechanism of diffusion process, so intraparticle diffusion model was investigated[52]. The intraparticle diffusion rules the adsorption process only when the plot is linear and passes through origin[46]. The adsorption process occurs in two stages, in the first stage the metal ions (chromium) move from solution into the adsorbent (MGO) surface known as film/external diffusion. During second stage, metal ions get into the pores on the surface of the adsorbent (MGO) and are said to be pore diffusion or surface diffusion[46,51,52]. In the present work, the obtained plot shows that the line does not pass through the origin and it attains lower correlation value (R^2=0.850 for chromium). With this reason it was state that intraparticle diffusion was not only the rate limiting step in the adsorption process of both the metal ion.

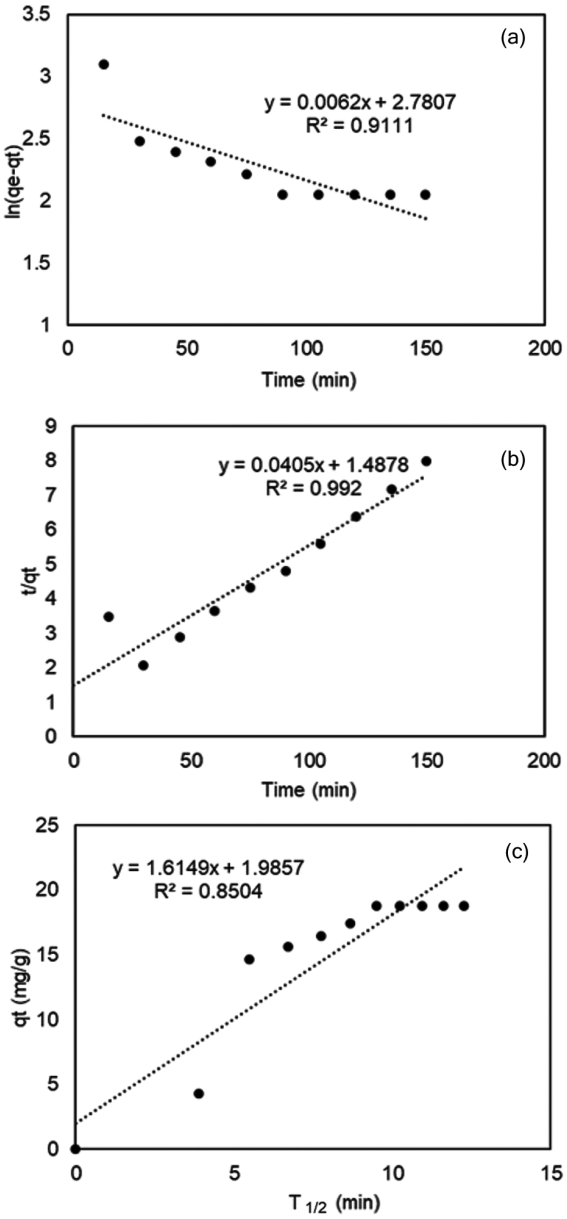

Fig. 7 — Adsorption kinetics exhibited by chromium on MGO adsorbent: (a) Pseudo first order (b) pseudo second order (c) intraparticle diffusion model

Adsorption isotherm modelling of chromium adsorption by MGO nanoadsorbent

Adsorption isotherm portrayed that the potential of the nanoadsorbent to interact with the metal ions and design the adsorption system can be done with the obtained data[50]. It describes the adsorption process, through by quantifying amount of adsorbed species to the concentration of the adsorbate at equilibrium condition[53]. In this research, adsorption isotherm studied for chromium and nickel ions onto MGO surface of the adsorbent with the optimised parameters. Commonly studied two parameter models namely Langmuir, Freundlich and Temkin were used to test the obtained data. The calculated parameters of their isothermal models are tabulated in the Table 4 and isothermal plots exhibited by chromium ions were

Table 3 — Kinetic study models with obtained constants by adsorption of chromium onto MGO surface

Type of kinetic model	Parameter	Value
Pseudo first order	Q_e(mg g^{-1})	1.613
	K_1(min^{-1})	0.043
	R^2	0.9111
Pseudo second order	Q_e(mg g^{-1})	2.469
	Q_e^2	610.09
	K_2(g mg^{-1} min^{-1})	0.027
	R^2	0.992
Intra particle diffusion	K_{diff}	1.614
	C	1.985
	R^2	0.850

Table 4 — Isotherm models with obtained parameters value by adsorption of chromium onto MGO surface

Type of isotherm	Parameter	Value
Langmuir	Q_{max} (mg g^{-1})	9.09
	K_L(L mg^{-1})	1.623^{E-06}
	R_L	0.999
	R^2	0.948
Freundlich	K_F	14.2
	$1/n$	1.0059
	R^2	0.996
Temkin	B_T(J mol^{-1})	7.79
	K_T (L mg^{-1})	0.0067685
	R^2	0.905

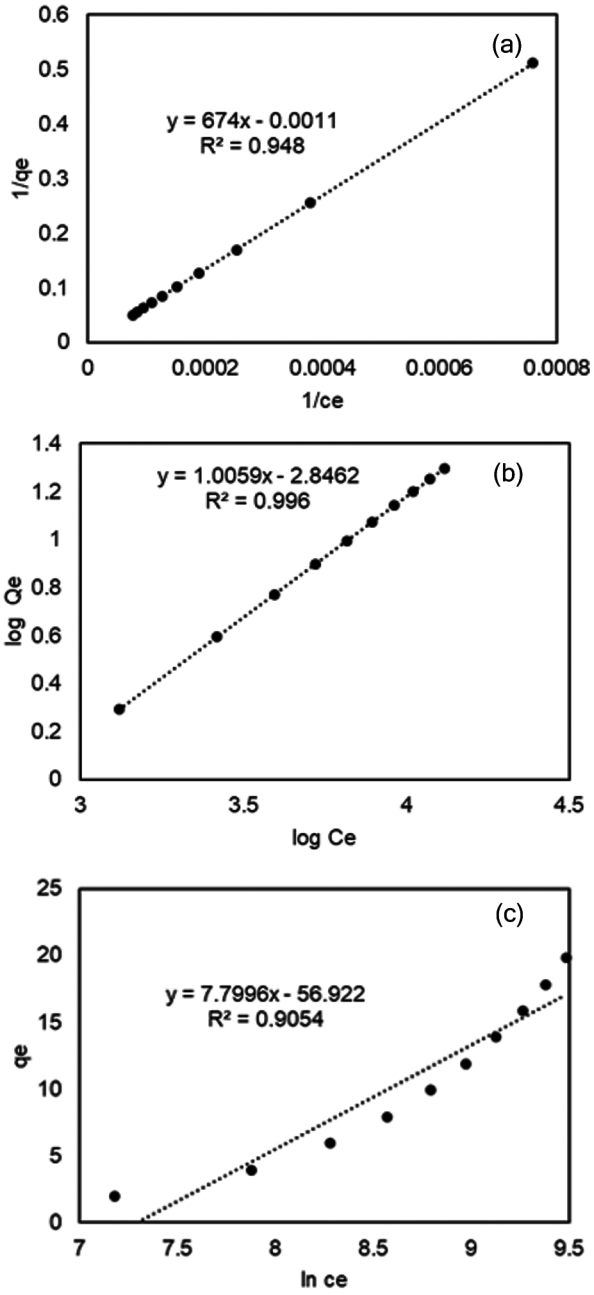

Fig. 8 — Adsorption isotherm exhibited by chromium on MGO adsorbent (a) Langmuir isotherm (b) Freundlich isotherm and (c) Temkin isotherm

shown in Fig. 8. The applicability and fitness of the model are predicted by the R^2 value[51]. The R^2 values of Langmuir, Freundlich and Temkin for chromium isotherm plots were 0.948, 0.996, 0.905, respectively. So, the fitness was in the order of Freundlich<Langmuir<Temkin. Hence, from the study it is to be stated that multilayer adsorption of chromium ions occurred onto heterogeneous surface of MGO. Freundlich was good fit and predicted to be multilayer adsorption of chromium ions onto MGO surface. The maximum adsorption capacity (q_{max}) was found to be 9.09 mg/g for chromium ions. The present results clearly indicated the excellent adsorption efficiency of MGO nanoadsorbent for wastewater treatment. Various adsorbents with q_{max} value obtained by other researchers in the literatures are mentioned in the Table 5 and through which we stated that our study obtained highest adsorption capacity for both chromium and nickel ions among the reports. The value of n indicates that physisorption occurred on heterogeneous surface of active sites on MGO by chromium ions, hence favourable for adsorption. Temkin does not favour the experimental data because of lower R^2 value.

Regeneration study

The resuscitation of adsorbent is an important parameter in the preparation of commercial adsorbent for industrial purpose. Desorbing agent with different concentration in the range of 0.1 to 2.0 M was tested, and the concentration at which highest desorption rate were selected for further study. In the present work, NaOH was used for chromium loaded adsorbent and the concentration was optimised from the obtained results shown in Fig. 9. The desorbing efficiency of the chromium loaded adsorbent was increased from 62.33 (0.2 M) to 98.09% (1.0 M), after which reduced and reached to 93.69% for 2.0 M NaOH. This is because the chromium ions were adsorbing highest in acidic conditions, so desorbed quickly in alkali solution[54], hence 1.0 M NaOH showed highest result. Here the MGO surface becomes negative and the chromium oxy-anions were easily desorbed which showed the ligand exchange reaction[46]. 1.0 M NaOH was decided to use for further regeneration cycles. Five cycles of adsorption were done to find its efficiency. The results indicated the chromium was desorbing from (1st cycle) 88.91 to 77.23% (5th cycle). Nearly, efficiency was reduced after five cycles for chromium, became 11.68% after the 5 cycles. Even after five cycles, the adsorbent magnetization was not reduced and between each cycle the dried adsorbent was weighed and noticed that there were no changes in weight. MGO @ poly (β-CD) was synthesised by Sun and his co-workers[55] and used HCl as eluent for desorption of Cd^{2+} and sulfamethazine and attained efficiency of adsorbents reduced only 13.35% after 6 cycles. Wang et al. [56] reported that the adsorbent MGO-PADP composite showed efficiency reduced to

Table 5 — Comparison on various adsorbents with its adsorption capacity

Sl. No.	Adsorbent	Adsorbate	Q_{max} (mg/g)	Reference
1.	GO-Fe_3O_4	Methylene blue and crystal violet	546.45 628.93	57
2.	GO-8-hydroxy quinolone	Cr (VI)	11.9	58
3.	Fe_3O_4	Pb^{2+}, Cr^{6+}	53.11 34.87	59
4.	GO/ Fe_3O_4/SO_3H	Cr^{6+}	222.22	60
5.	RGO/PEI/Fe_3O_4	Cr^{6+}	266.6	49
6.	PMGO	Cr(VI)	95.2	61
7.	GO, RGO	Ni^{2+}	90.8%, 84.4%	48
8.	GO-BPED-PS	Ni^{2+}, Co^{2+}	4.174±0.098 m mol/g, 3.902±0.092 m mol/g	42
9.	Fe_3O_4/GO/Chitosan (FGC Nanocomposite)	Ni^{2+}	12.24	62
10.	GO based hybrid membrane (GHMS)	Cu^{2+}, Co^{2+}, Ni^{2+},	4.338, 3.339, 3.160	27
11.	MGO	Pb^{2+}, Cr^{3+}, Cu^{2+}, Zn^{2+}, Ni^{2+}	200, 24.330, 62.893, 63.694, 51.020	64
12.	MGO(Natural graphite based)	Cr^{6+}	9.09	Present study

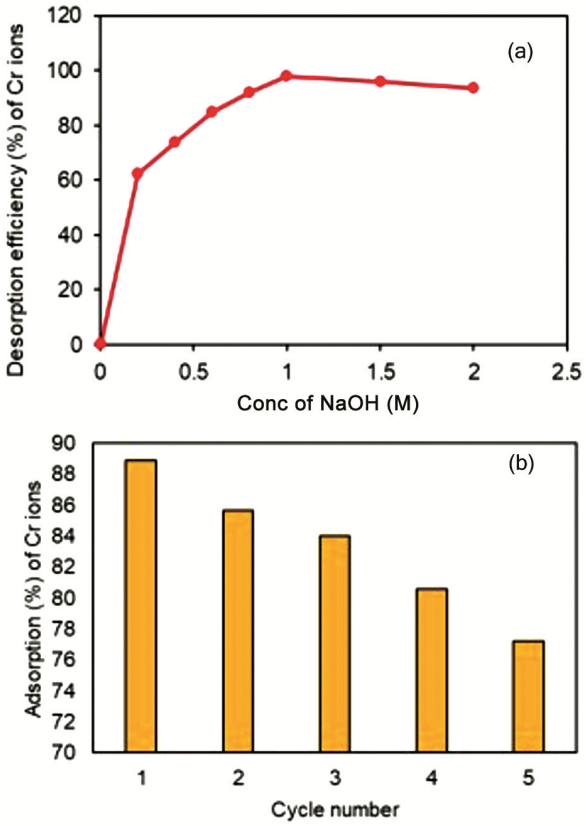

Fig. 9 — Desorption efficiency exhibited by chromium on MGO adsorbent: (a) Different concentration of NaOH on desorption efficiency of chromium ions and (b) number of cycles exhibited by chromium using MGO adsorbent

only 10.06% even after 5 cycles. Comparison of regeneration ability of various adsorbents with desorbing agent and its efficiency are tabulated in Table 6. Herein, our novel fabricated natural graphite made MGO can be reused up to five cycles of run and this eco-friendly adsorbent was really a promising solution to industrial wastewater treatment and water treatment.

Mechanism of formation of MGO from natural graphite using *S. potatorum* seeds

While synthesising GO by hummers method, here we avoided the use of $NaNO_3$ as it evolves toxic gas, which added advantage to this method. $KMnO_4$ helps in oxidation of graphite-to-graphite oxide and the H_2SO_4 added to the reaction to increases the oxidation efficiency of $KMnO_4$. Phosphoric acid was added for both increasing the acidity of the medium and oxidation efficiency. First, the natural graphite reacts with H_2SO_4 and forms H_2SO_4-graphite interaction and this increases the activity of graphite to oxidation process without affecting its structure. After the addition of $KMnO_4$, this H_2SO_4-graphite interaction starts oxidation and the mixture colour changes to green due to the presence of oxidizing agent Mn^{3+} and during the next step of heating this mixture to 55°C, which turns to dark brown colour indicating complete oxidation of graphite. In the chemical reaction process, the potassium permanganate reacts with sulphuric acid to produces dimanganese heptoxide (Mn_2O_7) and this selectively oxidized unsaturated aliphatic to aromatic double bonds which may have important implication in structure of graphite and its reaction pathways during oxidation. After the oxidation step over, the mixture was washed with three successive cycles of washing and before that permanganate and manganese residues were removed

Table 6 — Comparison of Regeneration capacity of various adsorbent with its desorbing agent, number of cycles and its removal efficiency

Sl. No.	Adsorbent	Adsorbate	Desorbing agent	Recovery (%)	No. of. cycles	Reference
1	MGO	Pb^{2+}, Cr^{3+}, Cu^{2+}, Zn^{2+}, Ni^{2+}	0.1 M HCl	87.51-78.12	4	64
2	GO-BPED GO-BPED-PS	Ni^{2+}, Co^{2+}	0.2 M EDTA, 0.2 M HCl, 0.2 M HNO_3	100-40, 100-65, 62-40	18	42
3	GO-C	MB,CV,Cu^{2+},Co^{2+}	10% HCl (10mL) + 1M NaOH (5mL)	95-97,92-98, 81-96,85-95	5	53
4	GO-PDAP/ Fe_3O_4	Pb^{2+}	1 M H_2SO_4	99-97	5	65
5	MGO @ Poly(-β CD)	Cd^{2+}, SMT	1 M HCl Ethanol	98-96 96-91	6	56
6	Fe_3O_4/GO/Chitosan (FGC Nano composite)	Ni^{2+}	0.1 M NaOH	83.03	3	62
7	MP BGO	Cu^{2+},$Co^{2+}$$Ni^{2+}$, Pb^{2+}	HNO_3	98-71,91-67, 92-69,98-68	3	66
8	EDA-MGO	Pb^{2+}	0.5 M HCl	98	5	67
9	NH_2-ASN, NH_2-MSN	Cr^{6+}	0.1 M HCl	61.9-46.3, 76.8-57.8	5	68
10	MGO (Natural graphite based)	Cr^{6+} Ni^{2+}	1 M NaOH, 1 M HCl	88.91-77.23 90.03-72.86	5	Present study

by using H_2O_2. After washing, the remainder coagulates with ether and dried to obtain graphite oxide which disperses in water under sonication to form graphene oxide. Then the magnetic GO was formed by precipitation of Fe_3O_4 on GO sheets. Initially pH of Fe^{2+} and Fe^{3+} iron solutions at pH 4 and mixed with ultrasonicated GO solution by which the iron particles adsorbed onto nano GO sheets and forms MGO[23,33].

Conclusion

Natural graphite made magnetic graphene oxide was triumphantly prepared by utilising *Strychnous potatorum* seeds as carbon source. The prepared adsorbent was well characterised which proves its functionalisation and magnetization. The successful oxidation of GO sheets and well anchored iron oxide particles onto GO sheets was evident from SEM results. EDX spectrum showed higher amount of oxygen and carbon containing functional group which are responsible for binding of metal ions and paves way to remediation. Different parameters were optimised and the results showed that the adsorption efficiency and its capacity will depend on these parameters. Increase in the initial concentration of metal ion and adsorbent dose lead to decrease the adsorption efficiency and capacity for chromium ions. The adsorption process was pH dependent and optimised as 2.0 for chromium ions and the equilibrium time for maximum adsorption of chromium was found to be 50 min, with 97.1% of removal. The isothermal study reveals that adsorption of chromium was fitted to Freundlich isotherm and the maximum capacity obtained to be 9.09 mg/g. The kinetic data follows pseudo second order, and the adsorbent surface becomes heterogeneous with multilayer, and favourable for adsorption. MGO showed super-eminent regeneration ability and can be used upto 5 cycles. This study suggests that this new, novel, green MGO adsorbent having potency of high removal rate, easily separated from solution after the process, can be reused. Stable and eco-friendly nature are the valuable qualities of our adsorbent which recommend its use for wastewater treatment.

Acknowledgement

Nanotechnology Research Centre (NRC), SRMIST is gratefully acknowledged for providing the research facilities like FTIR, UV-visible, VSM, and XRD. Sophisticated instrument facility SAIF-IITM, at IIT-Madras are also acknowledged for providing research facility for SEM analysis.

References

1 Baragano D, Forjan R, Welte L & Gallego J R, Nanoremediation of As and metals polluted soils by means of graphene oxide nanoparticles, *Sci Rep*, 10 (2020) 1896.

2 Janani R, Basker G, Siva Kumar K, Varajani S, Hao Ngo H & Gnansounou E, Advancements in heavy metals removal from effluents employing nano-adsorbents: Way towards cleaner production, *Environ Res*, 203 (2022) 111815.

3 Al-Sherbini A A, Ghannam H A A, El-Ghanam G M A, El-Ella A A & Youssef A M, Utilization of chitosan/Ag bionanocomposites as eco-friendly photocatalytic reactor for Bactericidal effect and heavy metals removal, *Heliyon*, 5 (2019) e01980.

4 Donga C, Mishra S B, Abd-El-Aziz A S & Mishra A K, Advances in graphene-based magnetic and graphene-based/TiO_2 nanoparticles in the removal of heavy metals and organic pollutants from industrial wastewater, *J Inorg Organmet Polym Mater*, 31 (2020) 463.

5 Sun Y, Liu X, Lv X, Wang T & Xue B, Synthesis of novel lignosulfonate-modified graphene hydrogel for ultrahigh adsorption capacity of Cr(VI) from wastewater, *J Clean Prod*, 295 (2021) 126406.

6 Thiruchelvi M, Senthamilselvi M M, Venkatraman B R, Arivoli S & Muruganantham N, Adsorptive removal of ferrous ion by activated *Borassus flabellifer* bark nano carbon – kinetic and thermodynamic studies, *Int J Pharm Biol Sci*, 8 (2018) 434.

7 Kulkarni R M, Dhanyashree J K, Varma E & Sirivibha S P, Batch and continuous packed bed column studies on biosorption of nickel(II) by sugarcane bagasse, *Results Chem*, 4 (2022) 100328.

8 Rahulan M K S K, Sujatha R A & Little F N A, Adsorption of hexavalent chromium from water using graphene oxide/zinc molybdate nanocomposite: Study of kinetics and adsorption isotherms, *Front Energy Res*, 11 (2023) 1139604.

9 Fito J, Abewaa M & Nkambule T, Magnetite-impregnated biochar of Parthenium hysterophorus for adsorption of Cr(VI) from tannery industrial wastewater, *Appl Water Sci*, 13 (2023) 78.

10 Yahya M D, Aliyu A S, Obayomi K S, Olugbenga A G & Abudulahi U B, Column adsorption study for the removal of chromium and manganese ions from electroplating wastewater using cashew nutshell adsorbent, *Cogent Eng*, 7 (2020) 1748470.

11 Vishnu D & Dhandapani B, Evaluation of column studies using Cynodon dactylon plant-mediated amino-grouped silica-layered magnetic nanoadsorbent to remove noxious hexavalent chromium metal ions, *IET Nanobiotechnol*, 15 (2021) 402.

12 Chigova J T & Mudono S, Adsorption of Chromium(VI) Using Nano-ZnO doped scrap tire-derived activated carbon, *J Geosci Environ Prot*, 10 (2022) 121.

13 Choudhury T R, Rahman M S, Liba S I, Islam A, Quraishi S B, Begum B A, Mustafa A I & Amin M N, Adsorptive removal of chromium from aqueous solutions using flax (Linum usitatissimum): Kinetics and equilibrium studies, *J Environ Chem Ecotoxicol*, 4 (2022) 132.

14 Huang H, Wang Y, Zhang Y, Niu Z & Li X, Amino-functionalized graphene oxide for Cr(VI), Cu(II), Pb(II) and Cd(II) removal from industrial wastewater, *Open Chem*, 18 (2020) 97.

15 Faiz M A, Azurahanim C C, Yazid Y, Suriani A B & Ain M S, Preparation and characterization of graphene oxide from tea waste and it's photocatalytic application of TiO_2/graphene nanocomposite, *Mater Res Exp*, 7 (2020) 015613.

16 Kaviyarasan G, Rahale C S, Shanmugasundaram R, Palaniselvam V & Saranya N, Biosynthesis of graphene oxide nanoparticles from coconut fronds, *Int J Environ Clim*, 13 (2023) 3007.

17 Thangaraj B, Mumtaz F, Abbas Y, Anjum D H, Solomon P R & Hassan J, Synthesis of graphene oxide from sugarcane dry leaves by two-stage pyrolysis, *Molecules*, 28 (2023) 3329.

18 Gado M A, Sorption of thorium using magnetic graphene oxide polypyrrole composite synthesized from natural source, *Sep Sci Tech*, 53 (2018) 2016.

19 Nasir S, Hussein M Z, Yusof N A & Zainal Z, Oil palm waste-based precursors as a renewable and economical carbon sources for the preparation of reduced graphene oxide from graphene oxide, *Nanomaterials*, 7 (2017) 182.

20 Akhavan O, Bijanzad K & Mirsepah A, Synthesis of graphene from natural and industrial carbonaceous wastes, *RSC Adv*, 4 (2014) 20441.

21 Omar H, Malek N S, Nurfazianawatie M Z, Rosman N F, Bunyamin I, Abdullah S, Khusaimi Z, Rusop M & Asli N A, A review of synthesis graphene oxide from natural carbon based coconut waste by Hummer's method, *Mater Today Proc,*75 (2023)188.

22 Li C, Chen D, Ding J & Shi Z, A novel hetero-exopolysaccharide for the adsorption of methylene blue from aqueous solutions: Isotherm, kinetic, and mechanism studies, *J Clean Prod*, 265 (2020) 121800.

23 Neolaka Y A B, Lawa Y, Naat J N, Riwua A A P, Iqbal M, Darmokoesoemoc H & Kusuma H S, The adsorption of Cr(VI) from water samples using graphene oxide-magnetic (GO-Fe_3O_4) synthesized from natural cellulose-based graphite (kusambi wood or Schleichera oleosa): Study of kinetics, isotherms and thermodynamics, *J Mater Res Technol*, 9 (2020) 6544.

24 Chen Y & He L, Preparation and adsorption properties of the graphene modified by magnetic nanoparticles, *World Sci*, 9 (2019) 1940008.

25 Rukman N K, Jannatin M, Supriyanto G, Fahmi M Z & Ibrahim W A W, GO-Fe_3O_4 Nanocomposite from coconut shell: Synthesis and characterization, *IOP Conf Series: Earth Environ Sci*, 217 (2019) 012008.

26 Hu Z, Zhang X, Li J & Zhu Y, Comparative study on the regeneration of Fe_3O_4@graphene oxide composites, *Front Chem*, 8 (2020) 150.

27 Li Y, Zhang X, Zhang P, Liu X & Han L, Facile fabrication of magnetic bio-derived chars by co-mixing with Fe_3O_4 nanoparticles for effective Pb^{2+} adsorption: Properties and mechanism, *J Clean Prod*, 262 (2020) 121350.

28 Patchaiyappan A, Sarangapany S, Saksakom Y A & Devipriya S P, Feasibility study of a point of use technique for water treatment using plant-based coagulant and isolation of a bioactive compound with bactericidal properties, *Sep Sci Technol*, 55 (2018) 112.

29 Madhavan S A K S & Karpagam S, Natural coagulants: An easy way to remove heavy metals from tannery effluents, *J Ind Pollut Control*, 35 (2019) 2266.

30 Kumar P S, Vaibhav K N, Rekhi S & Thayagarajan A, Removal of turbidity from washing machine discharge using Strychnos potatorum seeds: Parameter optimization and mechanism prediction, *Resour Effic Technol*, (2016) S171.

31 Koul B, Bhat N, Abubaker M, Mishra M, Arukha A P & Yadav D, Application of natural coagulants in water treatment: A sustainable alternative to chemicals, *J Water*, 14 (2022) 3751.

32 Nagaraja K, Rao K M, Hemalatha D, Zo S, Han S S & Krishnan Rao K S V, Strychnos potatorum L. Seed

polysaccharide-based stimuli-responsive hydrogels and their silver nanocomposites for the controlled release of chemotherapeutics and antimicrobial applications, *ACS Omega*, 7 (2022) 15.

33 Santamaria-Juarez G, Gomez-Barojas E, Quiroga-Gonzalez E, Sanchez-Mora E, Quintana-Ruiz M & Santamaria-Juarez J D, Safer modified Hummers' method for the synthesis of graphene oxide with high quality and high yield, *Mater Res Express*, 6 (2020) 12.

34 Falih M S, Mahdi S A & Merza M M, Study of removing of the hexavalent chromium ion from aqueous solutions using coal and Ficus modified, *Syst Rev Pharm*, 11 (2020) 1915.

35 Kalam S, Abu-Khamsin S A, Kamal M S & Patil S, Surfactant adsorption isotherms: A review, *ACS Omega*, 6 (2021) 32342.

36 Dinh H T, Tran N T & Trinh D X, Investigation into the adsorption of methylene blue and methyl orange by UiO-66-NO_2 Nanoparticles, *J Anal Chem*, 2021 (2021) 5512174.

37 Patra C, Shahnaz T, Subbiah S & Narayanasamy S, Comparative assessment of raw and acid-activated preparations of novel Pongamia pinnata shells for adsorption of hexavalent chromium from simulated wastewater, *Environ Sci Pollut Res*, 27 (2020) 14836.

38 Hieu N H, Nam H M & Hoai D P H, Fabrication, characterization, and adsorption capacity of Fe_3O_4/graphene oxide nanocomposites for nickel removal, *Sci Technol Stud*, 19 (2016) 1.

39 Hoan N T V, Thu N T A, Van Duc H, Cuong N D, Khieu D Q & Vo V, Fe_3O_4/reduced graphene oxide nanocomposite: Synthesis and its application for toxic metal ion removal, *J Chem*, 2016 (2016) 2418172.

40 Alberta E L, Che A C & Shiroshaki Y, Synthesis and characterization of graphene oxide functionalized with magnetic nanoparticle via simple emulsion method, *Results Phys*, 11 (2018) 944.

41 Andrade M B, Santos T R T, Silva M F, Vieira M F, Bergamasco R & Hamoudi S, Graphene oxide impregnated with iron oxide nanoparticles for the removal of atrazine from the aqueous medium, *Sep Sci Technol*, 54 (2018) 2653.

42 Chaabane L, Beyou E & Baouab M H V, Preparation of a novel zwitterionic graphene oxide-based adsorbent to remove of heavy metal ions from water: Modeling and comparative studies, *Adv Powder Technol*, 32 (2021) 2502.

43 Surendran G & Baral S S, Biosorption of Cr(VI) from wastewater using Sorghastrum Nutans L. Nash, *Chem Ecol*, 34 (2018) 762.

44 Enniya I, Rghioui L & Jourania A, Adsorption of hexavalent chromium in aqueous solution on activated carbon prepared from apple peels, *Sustain Chem Pharma*, 7 (2018) 9.

45 Yusuff A S, Adsorption of hexavalent chromium from aqueous solution by Leucaena leucocephala seed pod activated carbon: Equilibrium, kinetic and thermodynamic studies, *Arab J Basic Appl Sci*, 26 (2019) 89.

46 Pant B D, Neupane D, Paudel D R, Lohani P C, Gautam S K, Pokhrel M R & Poudel B R, Efficient biosorption of hexavalent chromium from water by modified arecanut leaf sheath, *Heliyon*, 8 (2022) e09283.

47 Li C, Chen D, Ding J & Shi Z, A novel hetero-exopolysaccharide for the adsorption of methylene blue from aqueous solutions: Isotherm, kinetic, and mechanism studies, *J Clean Prod*, 265 (2020) 121800.

48 Rajivgandhi G, Vimala R T V, Nandhakumar R, Murugan S, Alharbi N S, Kadaikunnan S, Khaled J M, Alanzi K F & Li W J, Adsorption of nickel ions from electroplating effluent by graphene oxide and reduced graphene oxide, *Environ Res*, 199 (2021) 111322.

49 Wang J, Zhang W & Wei J, Fabrication of poly(β-cyclodextrin)-conjugated magnetic graphene oxide by surface-initiated RAFT polymerization for synergetic adsorption of heavy metal ions and organic pollutants, *J Mater Chem A*, 7 (2019) 2055.

50 Yang J, Huang B & Lin M, Adsorption of Hexavalent chromium from aqueous solution by a chitosan/bentonite composite: Isotherm, kinetics, and thermodynamics studies, *J Chem Eng Data*, 65 (2020) 2751.

51 Darweesh M A, Mahmoud Y E, Mohamed I A, Abdel M M A, Elsayed N M K & Hammad W A, Adsorption isotherm, kinetic, and optimization studies for copper(II) removal from aqueous solutions by banana leaves and derived activated carbon, *South African J Chem Eng*, 40 (2022) 10.

52 Safwat S M, Mohamed N Y, Meshref M N A & Elawwad A, Adsorption of phenol onto aluminum oxide nanoparticles: Performance evaluation, mechanism exploration, and principal component analysis (PCA) of thermodynamics, *Adsorp Sci Technol*, 2022 (2022) 1924117.

53 Abd-Elhamid A L, Abu Elgoud, E M, Emam S H S H & Aly H F, Superior adsorption performance of citrate modified graphene oxide as nano material for removal organic and inorganic pollutants from aqueous solution, *Sci Rep*, 12 (2022) 9204.

54 Rai M K, Giri B S, Nath Y, Bajaj H, Soni S, Singh R P, Singh R S & Rai B N, Adsorption of hexavalent chromium from aqueous solution by activated carbon prepared from almond shell: Kinetics, equilibrium and thermodynamics study, *J Water Supply: Res Technol-AQUA*, 67 (2018) 724.

55 Wang Z, Wu Q, Zhang J, Zhang H, Feng J, Dong S & Sun J, In situ polymerization of magnetic graphene oxide-diaminopyridine composite for the effective adsorption of Pb(II) and application in battery industry wastewater treatment, *Environ Sci Pollut Res*, 26 (2019) 33427.

56 Wang D, Zhang G, Zhou L, Wang M, Cai D & Wu Z, Synthesis of a multifunctional graphene oxide-based magnetic nanocomposite for efficient removal of Cr(VI), *Langmuir*, 33 (2017) 7007.

57 Pu S, Xue S, Yang Z, Hou Y, Zhu R & Chu W, In situ co-precipitation preparation of a superparamagnetic graphene oxide/Fe_3O_4 nanocomposite as an adsorbent for wastewater purification: synthesis, characterization, kinetics, and isotherm studies, *Environ Sci Pollut Res*, 25 (2018) 17310.

58 Sheikhmohammadi A, Mohseni S M, Godini H, Sardar M, Abtahi M, Mahdavi S, Rezaei S, Dahaghin Z, Atafar Z, Almasian M, Sarkhosh M, Vosoughi M & Yaghobinejad R, Application of graphene oxide modified with 8-hydroxyquinoline for the adsorption of Cr(VI) from wastewater: Optimization, kinetic, thermodynamic and equilibrium studies, *J Mol Liq*, 233 (2017) 75.

59 Rajput S, Pittman C U & Mohan D, Magnetic magnetite (Fe_3O_4) nanoparticle synthesis and applications for lead (Pb^{2+}) and chromium (Cr^{6+}) removal from water, *J Colloid Interface Sci*, 468 (2016) 334.

60 Alizadeh A, Abdi G, Khodaei M M, Ashokkumar M & Amirian J, Graphene oxide/Fe_3O_4/SO_3H nanohybrid: A new adsorbent for adsorption and reduction of Cr(VI) from aqueous solutions, *RSC Adv*, 7 (2017) 14876.

61 Li N, Yue Q, Gao B, Xu X, Kan Y & Zhao P, Magnetic graphene oxide functionalized by poly dimethyl diallyl ammonium chloride for efficient removal of Cr(VI), *J Taiwan Inst Chem Eng*, 91 (2018) 499.

62 Tran L T, Tran H V, Le T D, Bach G L & Tran L D, Studying Ni(II) adsorption of magnetite/graphene oxide/chitosan nanocomposite, *Adv Polym Technol*, 2019 (2019) 8124351.

63 Dou W, Liu J & Li M, Competitive adsorption of Cu^{2+} in Cu^{2+}, Co^{2+} and Ni^{2+} mixed multi–metal solution onto graphene oxide (GO)–based hybrid membranes, *J Mol Liq*, 322 (2020) 114516.

64 Ain Q U, Farooq M U & Jalees M I, Application of magnetic graphene oxide for water purification: Heavy metals removal and disinfection, *J Water Process Eng*, 33 (2020) 101044.

65 Wang J, Zhang W & Wei J, Fabrication of poly(β-cyclodextrin)-conjugated magnetic graphene oxide by surface-initiated RAFT polymerization for synergetic adsorption of heavy metal ions and organic pollutants, *J Mater Chem A*, 7 (2019) 2055

66 Uogintė I, Lujanienė G &Valiulis D, Removal of heavy metals from contaminated water using nano-magnetic Prussian blue based on graphene oxide sorbent,.*Proceedings of ENVIRA*, (2019) 85.

67 Zarenezhad M, Zarei M, Ebratkhahan M & Hosseinzadeh M, Synthesis and study of functionalized magnetic graphene oxide for Pb removal from wastewater, *Environ Technol Innov*, 22 (2021) 101384.

68 Jang E H, Pack S P & Kim Chung S, A systematic study of hexavalent chromium adsorption and removal from aqueous environments using chemically functionalized amorphous and mesoporous silica nanoparticles, *Sci Rep*, 10 (2020) 55.